

RSC Advances



This is an *Accepted Manuscript*, which has been through the Royal Society of Chemistry peer review process and has been accepted for publication.

Accepted Manuscripts are published online shortly after acceptance, before technical editing, formatting and proof reading. Using this free service, authors can make their results available to the community, in citable form, before we publish the edited article. This *Accepted Manuscript* will be replaced by the edited, formatted and paginated article as soon as this is available.

You can find more information about *Accepted Manuscripts* in the [Information for Authors](#).

Please note that technical editing may introduce minor changes to the text and/or graphics, which may alter content. The journal's standard [Terms & Conditions](#) and the [Ethical guidelines](#) still apply. In no event shall the Royal Society of Chemistry be held responsible for any errors or omissions in this *Accepted Manuscript* or any consequences arising from the use of any information it contains.

Cite this: DOI: 10.1039/c0xx00000x

www.rsc.org/xxxxxx

FULL PAPER

For Table of Contents use only

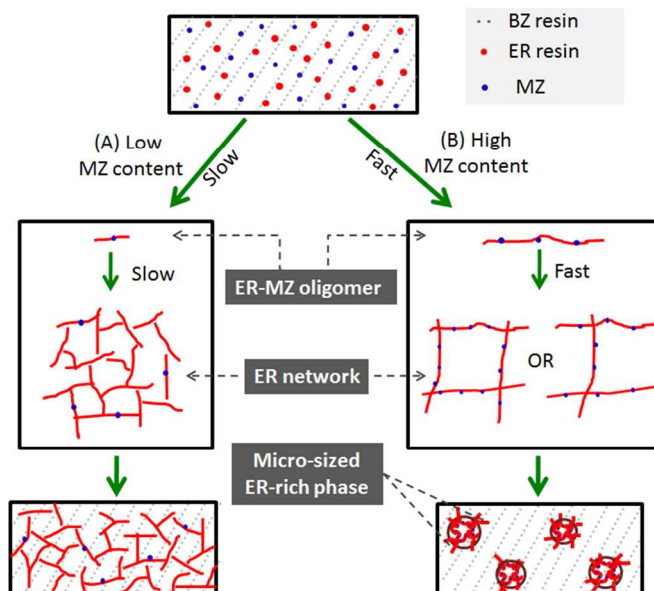
Reaction induced phase separation in thermosetting/thermosetting blends: Effects of imidazole content on the phase separation of benzoxazine/epoxy blends

5 Pei Zhao, Qian Zhou, Yu Yuan Deng, Rong Qi Zhu, Yi Gu*

Received (in XXX, XXX) Xth XXXXXXXXXX 20XX, Accepted Xth XXXXXXXXXX 20XX

DOI: 10.1039/b000000x

10 Multiphase structure were prepared in-situ in traditional homogeneous benzoxazine/epoxy blending systems by reaction induced phase separation method.



Cite this: DOI: 10.1039/c0xx00000x

www.rsc.org/xxxxxx

FULL PAPER

Reaction induced phase separation in thermosetting/thermosetting blends: Effects of imidazole content on the phase separation of benzoxazine/epoxy blends†

Pei Zhao, Qian Zhou, Yu Yuan Deng, Rong Qi Zhu, Yi Gu*

5 Received (in XXX, XXX) Xth XXXXXXXXXX 20XX, Accepted Xth XXXXXXXXXX 20XX

DOI: 10.1039/b000000x

Micro-sized phase separation structure was successfully realized in normally homogeneous benzoxazine (BZ)/epoxy (ER) (mass ratio: 80/20) blending systems in-situ by enhancing the content of catalyst, imidazole (MZ). To reveal the internal relationships between the content of MZ and the phase separation, 10 the phase morphology, polymerization activity, rheology and relaxation behaviors of BZ/ER blends with different contents of MZ were investigated by means of turbidity observation, scanning electron microscope (SEM), differential scanning calorimetry (DSC), rheological and dynamic mechanical thermal analysis (DMA), respectively. The results showed that in BZ/ER/MZ blending system, when the content of MZ was high enough (≥ 8 wt %), micro-sized ER-rich domains could be obtained, otherwise 15 homogeneous structure was obtained. What's more, the curing reaction of BZ/ER/MZ blends at 110 °C mainly associated with the polymerization of ER with MZ. Increasing the MZ content not only enlarged the reactivity difference between ER and BZ and accelerated the gelation, but also resulted in a branched or looser ER networks and relative low system viscosity, therefore was beneficial to phase separation.

1. Introduction

20 In the past few decades, thermosetting (TS) / thermosetting (TS) blending systems have attracted more and more attention due to their widely application in adhesives, filler-reinforced composite materials, automotive and aircraft components, and coatings for electronic circuits.¹⁻² However, because of the highly crosslinked 25 network structures, TS/TS blending systems are brittle materials that show unsatisfying toughness and elongation at break. Effective toughening strategies are of high interest to enable powerful new applications. It is well known that the properties of polymer blends are not only associated with their chemical 30 structures but also to their phase structures.³⁻⁵ For multi-component polymer systems, the introduction of multiphase structures can greatly improve the toughness of the products without sacrificing the other excellent properties, such as modulus and thermal mechanical properties, which is an 35 interesting modification method used in the polymer industry.⁶ Therefore the introduction of multiphase structures in the TS/TS blends was supported to be a good way to improve the toughness. As one of the method to introduce multiphase structures in multi-component polymer systems, reaction-induced phase separation, 40 which is designed as the uniform precursor system undergoing a phase separation into a two phase separated structure during the development of the curing process, has attracted much attention. This method has been widely used in the thermoplastic (TP) modified TS resin systems,^{3,7-9} but was fewly reported in TS/TS 45 blending systems.¹⁰ For TS/TP blends, such as epoxy/poly (ether imide) blends,¹¹ because there is much difference between TP

resin and TS precursor on their thermodynamic compatibility and initial dynamic asymmetry (such as, molecular weight (M_n), viscosity and glass transition temperature (T_g)), the entropy of 50 mixing as well as the compatibility can be significantly reduced with the curing reaction of TS resin.¹² While for TS/TS blends, such as benzoxazine/epoxy blending system,¹³ because the two components have good compatibility and are initial dynamic symmetry (e.g. similar low M_n , low viscosity and T_g), the initial 55 entropy of mixing is huge, which makes it difficult to get phase separation structure. In addition, in TS/TS blends, mutual entanglement of polymer chains in the cross-linked networks or the copolymerization between the two components always leads to the formation of permanent interlocked homogeneous 60 structures.

Accordingly, increasing the dynamic asymmetry during the curing reaction process and reducing the mutual entanglement as well as the copolymerization reaction are promising strategies to get phase separation structures in TS/TS blending systems. 65 Among the ways to increase the dynamic asymmetry, sequential polymerization of different component in the blending systems which has been reported previously, will be a good choice.¹⁴⁻¹⁶ The sequential polymerization refers to that one component (component A) can polymerize to a certain degree before another 70 one (component B) starts to polymerize in the presence of curing reagent. During this process, the M_n difference between the two components can be gradually enlarged and the systemic entropy of mixing can be significantly decreased, which will promote the phase separation of component A from matrix B. Through this 75 method, Yang and Dean etc. have obtained phase separation

structures in urethane/acrylate resin and epoxy/methacrylic acid blending systems, respectively.¹⁴⁻¹⁵ However, it should be noted that in their systems, the polymerization mechanisms between the two components are largely different (e.g. photo-initiated and thermal-initiated) and no copolymerization between the two components exists.

Nevertheless, it is well known that the occurrence of phase separation in multi-component blending system depends on the competition effect between the kinetics of thermodynamic driving force for phase separation and cross-linking reaction of the polymerization component.⁷ In TS/TS (A/B) blending system, the preferential polymerization of A resin will increase the M_n of polymer A, thus enlarge the dynamic asymmetry between A and B resin and increase the thermodynamic driving force for phase separation, which is beneficial to phase separation. On the other hand, the crosslinking reaction of A resin will lead to vitrification and the increment of viscosity of A/B blending system, which will inhibit phase separation. Therefore, how to balance the opposite effects of curing reaction of A resin on the phase separation is the key to get multi-phase separation structures in TS/TS blending systems.

Due to the good processability, excellent thermal and physical mechanical properties, benzoxazine (BZ)/ epoxy (ER) blending system has attracted much more attention in the past decades.¹⁷ Herein, BZ/ER blending system is chosen as an example to study the phase separation of TS/TS blending systems. Ishida and Rimdusit et al. studied the curing behaviour of BZ/ER binary blending system and reported that the phenolic hydroxyl groups (-OH) produced by the ring-opening polymerization of BZ could initiate the polymerization of epoxy groups,^{13,18-20} leading to the copolymerization between BZ and ER. Besides, the curing mechanisms of BZ and ER resin both belong to ring-opening mechanism,²¹⁻²² most of the ER polymerization catalysts (or initiators), such as Lewis acids,²³⁻²⁴ imidazole,²⁵⁻²⁷ tertiary amine²⁸⁻²⁹ and organic acids³⁰, etc. can also be used to catalyze the polymerization of BZ resin.³¹⁻³⁷ Consequently, it was relatively difficult to precisely control the polymerization sequence of BZ and ER resin via catalyst design and no phase separation phenomenon was reported in BZ/ER blending system.^{13,38-43} Until recently, Grishchuk et al occasionally observed nano-sized phase domains in BZ/ER/amine blending systems by atomic force microscope.^{34,44} However, no systematic investigations about the phase separation of the blending systems and their influencing factors were reported.

Our group has done a lot of contributions to develop phase separation structures in BZ/ER blends. We investigated the possibility of phase separation in BZ/ER blends by model component, and concluded that if epoxy resin can polymerize to long molecular chains before the polymerization of BZ resin, phase separation could be observed in BZ/ER blends. Besides, based on the long terms investigation about the catalytic polymerization of BZ and ER resin, we found that imidazole (MZ), a low temperature curing agent of ER resin, is a proper catalyst to realize the sequential polymerization of ER and BZ at proper initial curing temperatures (80 °C~140 °C).⁴⁵ Recently, using MZ as catalyst, we successfully prepared sea-island phase

morphology in BZ/ER blending systems at 110 °C via reaction-induced phase separation method.⁴⁶

To be honest, BZ/ER/MZ blending system has been investigated for a long term, but only homogeneous structure was reported.⁴⁵ Comparing the reported systems with our novel multiphase systems, we find that in the same BZ and ER mass ratio, MZ content is the critical factor that influencing the final structure. In this work, we devoted ourselves to reveal the internal relationship between MZ content and phase separation in BZ/ER/MZ blending systems. In order to do this, the influence of MZ content on the phase morphology, curing reactive of BZ and ER, and rheological behaviour were systematically investigated by means of differential scanning calorimetry (DSC), turbidity observation, scanning electron microscope (SEM), Fourier transform infrared (FTIR), rheological measurement and dynamic mechanical thermal analysis (DMA).

2. Experimental

2.1 Materials

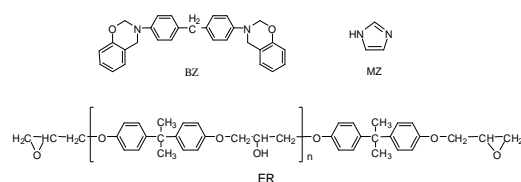
Benzoxazine resin (BZ), industrial grade, based on 4, 4'-diaminodiphenyl methane (DDM), phenol and paraformaldehyde was synthesized and characterized as previous report,⁴⁷ and was used without further purification. The average number molecular weight (M_n) of BZ resin was about 435 g mol⁻¹. Phenol, DDM and paraformaldehyde were purchased commercially from Chengdu Kelong Chemical Reagents Corp. (China) and used as received. Bisphenol-A-based ER (Commercial name E44), industrial grade, was provided by Shanghai synthetic resin factory (China) and had an epoxy equivalent weight of 227~246 g eq⁻¹. Phenol, DDM, paraformaldehyde, tetrahydrofuran (THF) and imidazole (MZ, melting temperature 91 °C) were supplied by Chengdu Kelong Chemical Reagents Corp. (China). The chemical structures of materials were shown in Scheme 1.

2.2 Preparation of BZ/ER/MZ blends

The blends of BZ/ER/MZ were prepared by mixing BZ and ER resin (mass ratio: 80/20) at 110 °C for 20min, and when the mixture was cooled to 95 °C, MZ was added and the mixture was stirred vigorously for 2 min until MZ completely dissolved. The samples were degassed under vacuum for another few minutes afterward and then refrigerated (-18 °C) to avoid any further curing reaction. Samples for BZ/MZ and ER/MZ were prepared by the same way.

The blends of BZ/ER/MZ involved in this work were defined as BZ/ER/MZ (3wt%), BZ/ER/MZ (8wt%) and BZ/ER/MZ (12wt%). Herein, the mass ratio of BZ and ER was fixed at 80:20, and the weight fraction of MZ was 3wt%, 8wt% and 12wt% of the content of ER, respectively.

Scheme 1. Chemical structures of BZ, ER and MZ.



Cite this: DOI: 10.1039/c0xx00000x

www.rsc.org/xxxxxx

FULL PAPER

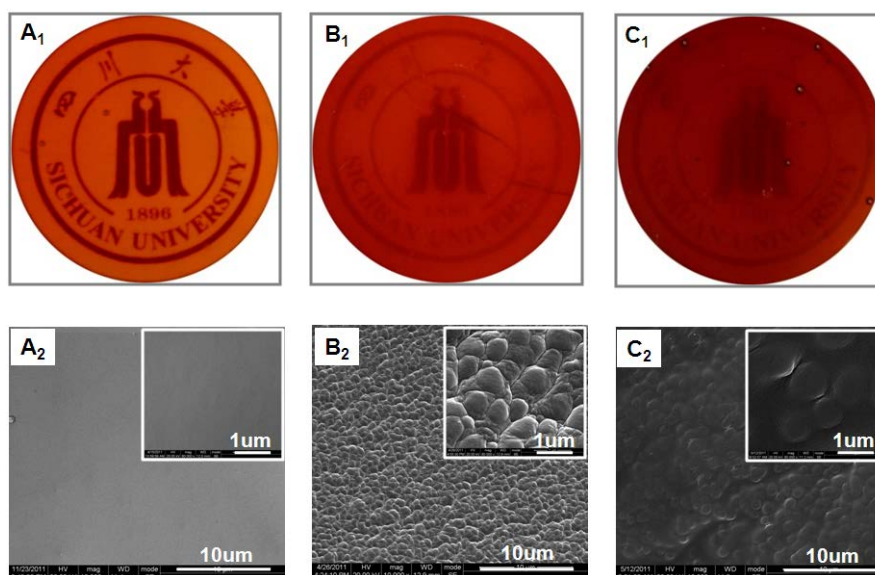


Figure 1. Transparency (A_1 , B_1 and C_1) and SEM (A_2 , B_2 and C_2) morphology of BZ/ER/MZ blends with 3 wt% (A_1 and A_2), 8 wt% (B_1 and B_2) and 12 wt% (C_1 and C_2) of MZ, respectively. Samples for transparency observation were cured at 110 °C for 5h, for SEM observation were etched with THF to remove BZ-rich phases after curing at 110 °C for 5h (A_2 and B_2) or 3h (C_2).

2.3 Measurement

Turbidity: In order to facilitate the observation of the turbidity of the blending system, the badge of Sichuan University was placed at the bottom of the reaction mould and pictures that reflected systemic states at specific curing stage were taken with a camera.

Scanning electron microscope (SEM): The phase morphology of the blend was investigated by field emission SEM (FEI Inspect F). Samples for SEM measurement were fractured under liquid nitrogen, and etched with THF at room temperature for 2~3 min. The fractured surfaces were dried at room temperature under vacuum and then coated with gold before SEM observation.

Differential scanning calorimetry (DSC): The curing reaction of the blends was investigated by DSC (TA Q20). The enthalpy was measured with the heating rate of 10 °C min⁻¹ from room temperature to 350 °C under nitrogen flow of 50 ml min⁻¹. Meanwhile, ramp scanning with different heating rates (5, 10, 15, and 20 °C min⁻¹) under N₂ atmosphere was done to investigate the apparent cure activation energy (E_a).

Fourier transform infrared (FTIR): The component of each rich phase was investigated by Fourier transform-infrared spectroscopy (FTIR) and ATR-FTIR measurements which were performed on a Nicolet 5700 FTIR spectrometer. Sample for FTIR was prepared by casting THF solutions onto potassium bromide window at room temperature. All of the spectra were obtained at a resolution of 4 cm⁻¹ and the average of 32 scans.

Rheological measurements: The rheological behaviours of the blends were recorded on an Ares-9A rheometry instrument. One geometry was chosen, namely, parallel plates with diameter 20mm (up) and 25mm (down). The isothermal temperature was

110 °C. The dynamic time sweep at a given temperature, pulsation (1 rad/s), and deformation (1%) was used in order to obtain steady state and thus ensure that measurements were performed under dynamic equilibrium conditions.

Dynamic mechanical thermal analysis (DMA): The relaxation behaviours were performed with TA Q800 DMA equipment. Specimens with the dimension of 30 × 10 × 3 mm³ were tested in three point bend mode. The maximum strain amplitude was 20 μm and the oscillating frequency was 1 Hz, as the temperature was scanned from 40 to 250 °C with the heating rate of 5 °C/min. Samples for DMA measurement were cured at 110 °C for 20h, and then 180 °C for 2h.

3. Result and Discussion

3.1 Turbidity and Morphology

For BZ/ER/MZ blends with different content of MZ, before the curing reaction, all the samples were homogeneous solutions with bright yellow appearance. After curing at 110 °C for 5h, the transparency of these samples became different: higher content of MZ in the blend, poorer transparency from the appearance (Figure 1 $A_1 \rightarrow B_1 \rightarrow C_1$). The turbid phenomenon indicated the occurrence of phase separation in BZ/ER/MZ blending system with 8wt% (B_1) and 12wt% (C_1) MZ. To further prove the phase separation structures, the fractured surfaces of half cured PBZ/ER/MZ blends were etched with THF and investigated by SEM. As shown in Figure 1, no phase separation was observed in the sample with 3wt% MZ (A_2), while clearly heterogeneous morphology with irregular spherical domains (0.8~1.2 μm)

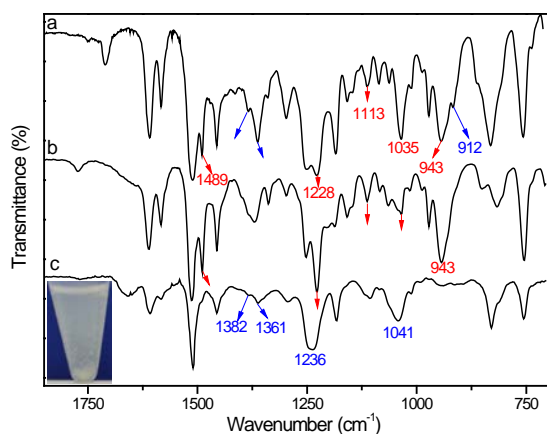


Figure 2. FTIR spectra of BZ/ER/MZ (8wt%) blend (a), and the THF-soluble part (b) and THF-insoluble part (c) of PBZ/ER/MZ blend after curing at 110 °C for 5h and etching with THF for 24h.

dispersed in the matrix was observed in the blends with 8wt% and 12wt% MZ (B₂ and C₂).

After etching with THF for 24h, the half cured phase separated PBZ/ER/MZ bulk gradually decomposed into a large amount of white insoluble floccules (Figure 2 insert). This phenomenon implies that the dispersed phase cannot dissolve in THF, while the matrix (continuous phase) is soluble in THF at the phase separation point. In order to distinguish the component of each rich phase, THF-soluble part and THF-insoluble part were run FTIR and ATR-FTIR scanning separately. Herein, BZ/ER/MZ (8 wt%) blend was selected as an example, and the FTIR spectrum of original BZ/ER/MZ (8 wt%) blend was shown in Figure 2a for comparison.

As shown in Figure 2a, the characteristic absorption bands of ER resin (912 cm⁻¹, epoxy group) and BZ resin (943 cm⁻¹, oxazine ring) were both observed in the FTIR spectrum. Meanwhile, the absorption bands of BZ resin at 1035 cm⁻¹ ($\nu_{s,C-O-C}$), 1228 cm⁻¹ ($\nu_{as,C-O-C}$), 1113 cm⁻¹ ($\nu_{as,C-N-C}$) and 1489 cm⁻¹ (1,2-disubstituted benzene) were also observed, which covered the characteristic absorption bands of ER resin at 1041 cm⁻¹ ($\nu_{s,C-O-C}$) and 1236 cm⁻¹ ($\nu_{as,C-O-C}$). In Figure 2b, all of the characteristic peaks of BZ monomer were found, indicating that the main component of THF-soluble part was unpolymerized BZ resin. While in Figure 2c, the disappearance of the peaks of BZ resin at 943 cm⁻¹ and 1489 cm⁻¹, and the observation of absorption bands of ER resin at 1382 cm⁻¹ and 1361 cm⁻¹ (δ_{C-H} of isopropyl structures), 1041 cm⁻¹ and 1236 cm⁻¹ indicated that the main component of THF-insoluble part was ER resin. The absence of characteristic absorption band of epoxy group at 912 cm⁻¹ revealed the complete polymerization of ER resin. Therefore, it could be concluded that the embossed dispersed domains observed in Figure 1 (B₂ and C₂) corresponded to ER-rich phases, and the continuous phase (matrix) corresponded to BZ-rich phases.

3.2 The curing reaction of BZ/ER/MZ

The curing reactions of BZ, ER and BZ/ER blend with or without MZ were investigated by DSC measurements. From Figure 3a and 3b, it is clearly that MZ can catalyze the polymerization of both ER and BZ resin, but the catalytic effect for ER resin was more obvious. For BZ/ER blend, only one exothermic peak at

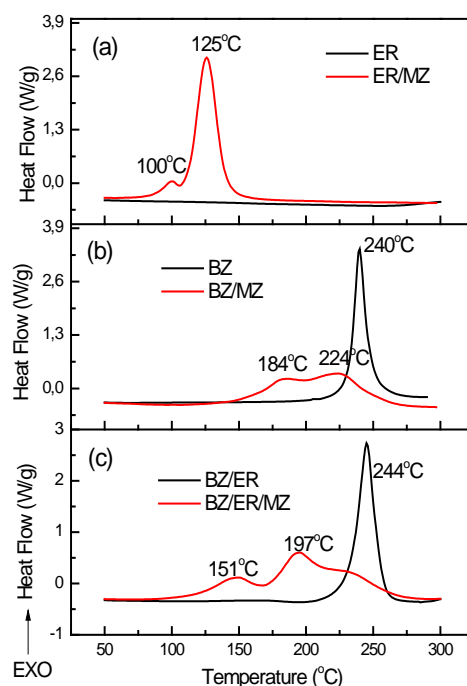


Figure 3. DSC curves of ER and ER/MZ (a), BZ and BZ/MZ (b), BZ/ER and BZ/ER/MZ (8 wt%) blends (c).

244 °C was observed, while under the catalysis of MZ (8 wt%), multi-peaks were observed and the peak temperatures were shifted toward low temperatures (Figure 3c). Compared with the DSC curves of ER/MZ and BZ/MZ blend, we deduced that in ternary blend the peak at low temperature (151 °C) corresponded to the polymerization of ER with MZ, and the peak at high temperature (197 °C) corresponded to the polymerization of BZ resin. This deduction was consistent with our previous reports.⁴⁶

3.3 Polymerization sequence

As shown in Figure 4, increasing the content of MZ, the exothermic peaks of BZ/ER/MZ blends shifted to low temperatures and the two peaks corresponding to the polymerization of ER and BZ resin were well separated. To further investigate the effect of MZ content on the polymerization of BZ and ER in ternary blending systems, the exothermic curves of BZ/ER/MZ blending systems were well fitted by four Gaussian functions.⁴⁹ Here, BZ/ER/MZ (8 wt%) blend was shown as an example to study the peak assignment (Figure 5). According to the above DSC results, peak 1 and 2 should correspond to the polymerization of ER resin, and peak 3 and 4 should correspond to the polymerization of BZ resin. Therefore, the reactivity difference between ER and BZ in BZ/ER/MZ blends was mainly dependent on the reactivity difference between the two adjacent peaks (peak 2 and peak 3).

In this study, the reactivity of ER and BZ resin in BZ/ER/MZ blending system was estimated by activation energy (E_a). To get the E_a information of the blending system, DSC measurements of a series of blends under different heating rates were carried out. The peak fitted temperatures corresponding to Peak2 and Peak3 were recorded and summarized in Table S1. According to the Ozawa equation:⁵⁰⁻⁵¹

Cite this: DOI: 10.1039/c0xx00000x

www.rsc.org/xxxxxx

FULL PAPER

Table 1. The relationship between E_a results and phase separation of BZ/ER/MZ blends

System	E_{a2} ^a (KJ mol ⁻¹)	E_{a3} ^a (KJ mol ⁻¹)	$\Delta E_a = (E_{a3} - E_{a2})/E_{a2}$	Phase Separation ^b
BZ/ER/MZ (3wt%)	78.1	105.2	34.7%	NO
BZ/ER/MZ (8wt%)	67.4	102.1	51.5%	Yes
BZ/ER/MZ (12wt%)	67.2	102.7	52.8%	Yes

^a Calculated by Ozawa equation.^b According to the turbidity observation and SEM morphology measurement.

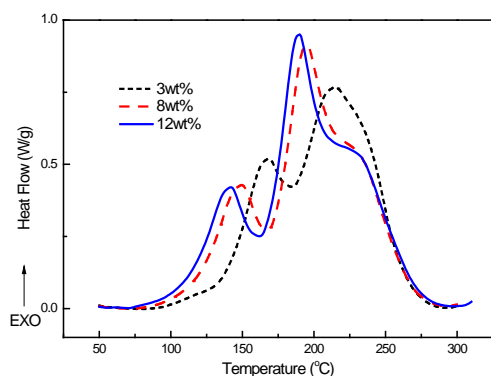
$$\ln\beta = C - 1.052 \times \frac{E_a}{RT_p}$$

Where, β is the heating rate, R is the gas constant, C is a constant parameter independent of E_a , and T_p is the peak temperature (K), the E_a of peak2 (E_{a2}) and peak3 (E_{a3}) were calculated from the resultant slope of $\ln\beta$ vs. $1/T_p$ (Figure S1) and summarized in Table 1.

As shown in **Table 1**, when the content of MZ increased from 3wt% to 12wt%, the E_a of ER (E_{a2}) decreased from 78.1 to 67.2 KJ mol⁻¹, while the E_a of BZ (E_{a3}) almost did not change (105.2~102.7 KJ mol⁻¹). That's to say, increasing the MZ content to some extent could improve the reactivity of ER, while had little effect on that of BZ resin, thus enlarged the reactivity difference ΔE_a between ER and BZ (from 34.7% to 52.8%). This result might be due to the fact that most of MZ has been consumed during the polymerization of ER/MZ, only small amount of MZ was left to catalytic the polymerization of BZ resin.

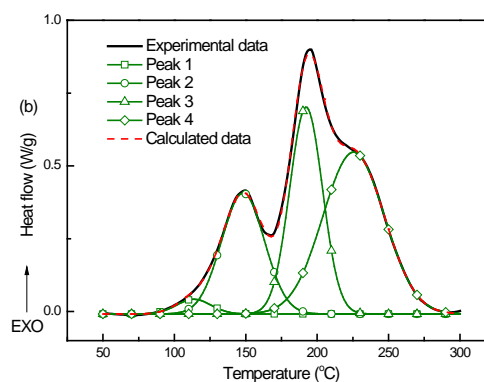
3.4 The growth of molecular chain during phase separation process

Figure 6A compared with the DSC curing exothermal curves of BZ/ER/MZ (8 wt%) blending system before and after curing at 110 °C for 5h. It was clear that, after curing at 110 °C for 5h, the peak at 151 °C corresponding to the polymerization of ER with MZ disappeared, while the peak at 197 °C corresponding to the polymerization of BZ resin almost had no change. Combining

**Figure 4.** DSC curves of BZ/ER/MZ blends with different contents of MZ.

with the conversion-time curves of BZ/ER and ER/MZ systems (Figure 6B), which showed that the conversion of BZ/MZ was less than 5% after curing at 110 °C for 30 min, while that of ER/MZ could rapidly reach to 80%, we concluded that the polymerization of BZ/ER/MZ blend at 110 °C was mainly associated with the polymerization of ER with MZ. In this case, the polymerization of ER with MZ played an important role for the phase separation of BZ/ER/MZ blends, for clear phase separation was observed after curing at 110 °C for 5h.

DSC curves of ER/MZ blends shown in Figure 7 manifested that ER has two exothermal peaks under the catalysis of MZ. Increasing the MZ content, both of the two peaks shifted towards low temperatures, and the peak area at low temperature increased. Heise⁵²⁻⁵³ and Vogt⁵⁴ et al. studied the polymerization of phenyl glycidyl ether (PGE) with 1,3-unsubstituted MZ and attributed the peak at the low temperature to the MZ: PGE (1:2) adduct formation (Scheme 2, step 1) and the main peak to the alkoxide-initiated polymerization (Scheme 2, step 2). Farkas and Strohm⁵⁵ proposed that MZ: PGE (1:2) adducts were assumed to act as the initiators for the polymerization of PGE by an etherification reaction in which the reactive alkoxide anion was the propagating species. Meanwhile, Barton et al. claimed that the adduct formation step and alkoxide-initiated polymerization of ER/MZ occurred step by step, but not simultaneously.⁵⁶ According to the reported polymerization mechanism of ER/MZ shown in Scheme 2, the adduct formation step tends to form a linear polymer, and the subsequent anionic polymerization causes the crosslinking

**Figure 5.** Peak fit results of the curing exothermal curves of BZ/ER/MZ (8 wt%) blend at the rate of 10 °C/min.

Cite this: DOI: 10.1039/c0xx00000x

www.rsc.org/xxxxxx

FULL PAPER

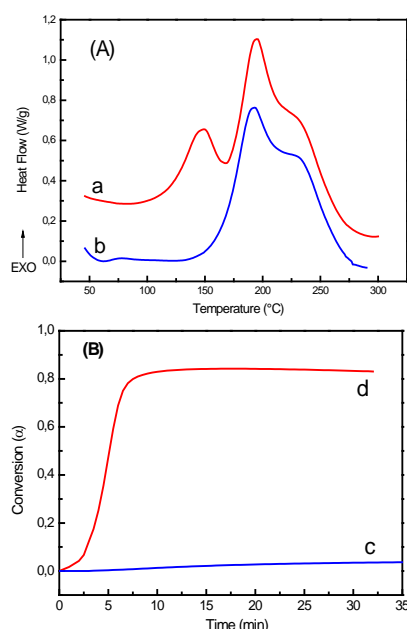


Figure 6. (A) DSC curves for BZ/ER/MZ blend with 8wt% of MZ before (a) and after (b) curing at 110 °C for 5h. (B) Isothermal conversion curves at 110 °C: (c) BZ with 3 wt% of MZ; (d) ER with 3 wt% of MZ.

reaction and leads to the formation of three dimensional network structure.²⁶ In this case, increasing the MZ content would form longer ER-MZ oligomers firstly, and then resulted in a looser network structures.

Figure 8 shows the storage modulus and tan delta curves of cured ER/MZ blends. The storage modulus (E_r) at the rubber plateau decreased with the increase of MZ content. According to the theory of rubber elasticity, the crosslinking density (ν) of effective network chains and the molecular weight between crosslinks (M_c) can be estimated from E_r , as¹³

$$E_r = 3\phi\nu RT = 3\phi \frac{\rho}{M_c} RT$$

Where ϕ is a front factor, which is unity for ideal rubbers (here we assumed $\phi = 1$), R is the gas constant, and E_r is the storage modulus at temperature T ($T_g + 30$ K), ρ is the bulk density of polymer (1.22 g/cm³ for ER/MZ). This equation is strictly valid only for lightly crosslinked materials and therefore is used only to qualitatively compare the level of crosslink.

As shown in Table 2, when the content of MZ increased from 1 wt% to 8 wt%, the crosslinking density of ER/MZ blends decreased from 11.6×10^3 to 0.9×10^3 mol/m³, and the molecular weight between crosslinks increased 12 times. This result confirmed that with high MZ content, the polymerization of ER was tend to form long linear ER polymer chains before the gelation, and then resulted in a looser network. Otherwise, the polymerization of ER was tend to form short polymer chains before the gelation, and resulted in a tight network.

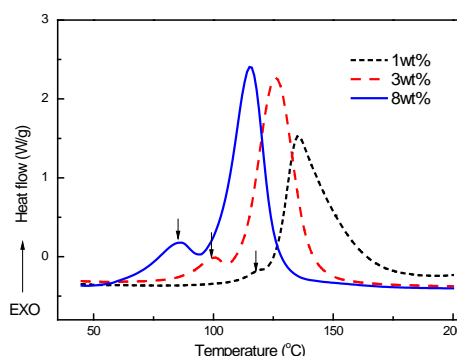


Figure 7. DSC curves of ER/MZ blend with different content of MZ.

3.5 Rheological behavior

The real-time isothermal (110 °C) rheological results for BZ/ER/MZ blending systems with different MZ content was measured and shown in Figure 9. As the gel point for thermosetting resin can be estimated from the crossover point of storage modulus (G' , elastic response) and loss modulus (G'' , viscous behavior) [57-58], it is clear that the gel time of BZ/ER/MZ blends decreased from 2646s to 1906s, and the viscosity at gel point increased 14 times as the content of MZ increased from 3wt% to 8wt%. While further increasing the MZ content to 12wt%, no gel point was observed ($G' > G''$ during the whole curing process), but high viscosity was obtained in a very short time (< 1500 s). What's more, the information about the increasing rate and the final viscosity of BZ/ER/MZ blends also were obtained from Figure 9B. For maximum content of MZ (c), the system viscosity had a rapid enhancement in a short time ($t < 1500$ s) and then balanced at 4969 Pa.s. For minimum content of MZ (a), the system viscosity increased very slowly at the initial stage ($t < 2000$ s), but underwent a rapid enhancement around the gel point and the final viscosity (76082 Pa.s) was 15 times higher than that of curve (c). As for the middle content of MZ (b), the above situation fell in between a and c.

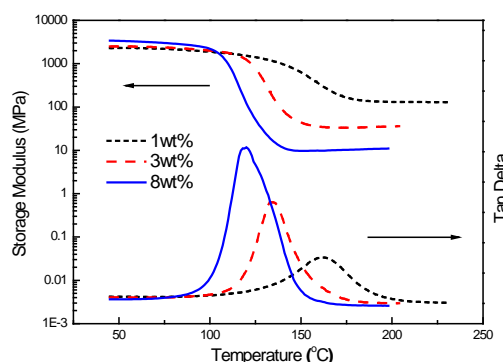


Figure 8. Storage modulus and tan delta curves of ER/MZ blend with different content of MZ after curing at 110 °C/20h + 180 °C/2h.

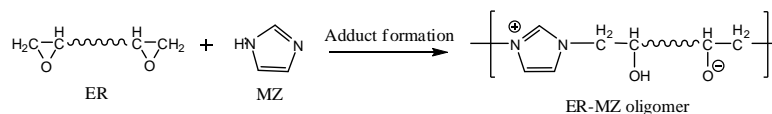
Cite this: DOI: 10.1039/c0xx00000x

www.rsc.org/xxxxxx

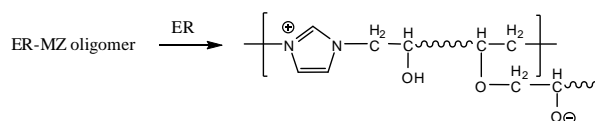
FULL PAPER

Scheme 2. Polymerization routes of ER in presence of MZ.

Step (1) Adduct formation



Step (2) Alkoxide initiated polymerization



From the above analysis, it was interesting to note that when the MZ content was high to 12wt%, no gelation phenomenon was observed. And increasing the content of MZ led to a fast increase of the viscosity and high viscosity before the gelation but a relatively lower viscosity at balanced domains. Because the curing reaction of BZ/ER/MZ blend at 110 °C was mainly associated with the polymerization of ER with MZ, the gelation and isothermal viscosity various both contributed to the polymerization of ER/MZ. In our systems, when the MZ content was 12wt%, the molar ratio of epoxy group of ER resin to the N function groups of MZ compound was 2.5/2.0. Most of the epoxy groups was consumed during the adduct formation process, and only few of them was left to take part in the crosslink reaction (alkoxide-initiated polymerization). That's why no gelation phenomenon could be observed in BZ/ER/MZ blend with 12wt% of MZ. This result indirectly proved that looser or linear/branched poly-ER would be obtained with the increase of MZ content, which was consistent with the results shown in Table 2. What's more, before the gelation, the fast increase of viscosity and the high viscosity value indicated the fast growth of the ER molecular chains and the formation of high molecular weight of linear ER-MZ oligomers, which decreased the system entropy of mixing, and increased the dynamic asymmetric between ER and BZ, thus favoring the occurrence of phase separation.¹⁵ Meanwhile, the relative low complex viscosity at balanced domains indicated the formation of branched or looser poly-ER network structures, which could allow the free diffusion of BZ monomers in and out of the ER network. Therefore, high MZ content was the key to balance the opposite influences of curing reaction of ER resin on the phase separation of BZ/ER/MZ blending system.

Table 2. DMA data for the cured ER/MZ blends

MZ content	E_r (MPa)	T_g^a (K)	ν (10^3 mol/m ³)	M_c (g/mol)
1wt%	134.5	434.0	11.6	105.2
3 wt%	33.9	407.5	3.1	393.5
8 wt%	9.7	392.3	0.9	1355.6

^a Peak temperature of $T_{\tan \delta}$

3.6 Phase separation process

According to the results and discussions given in the previous sections, the relationships among MZ content, curing reaction, rheological behavior and the phase separation of BZ/ER/MZ blending system were obtained as illustrated in Scheme 3.

Before the curing reaction, BZ resin, ER resin, and MZ were homogeneously mixed. When the reaction started at 110 °C, ER resin could homopolymerize preferentially under the catalyst of MZ to form linear ER-MZ oligomers and then to form branched or crosslinked ER networks. But the ER network structures and the final morphology of PBZ/ER/MZ blends were depended on the MZ content added in the system:

(A) If the MZ content was low (≤ 3 wt%), the molecular chain of ER-MZ oligomer formed in the first step shown in Scheme 1 was much shorter, which led to the formation of much tighter ER-network in the following alkoxy-anion-initiated polymerization of

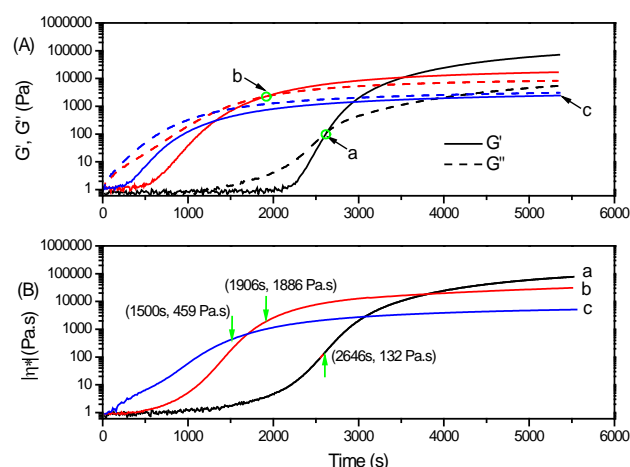
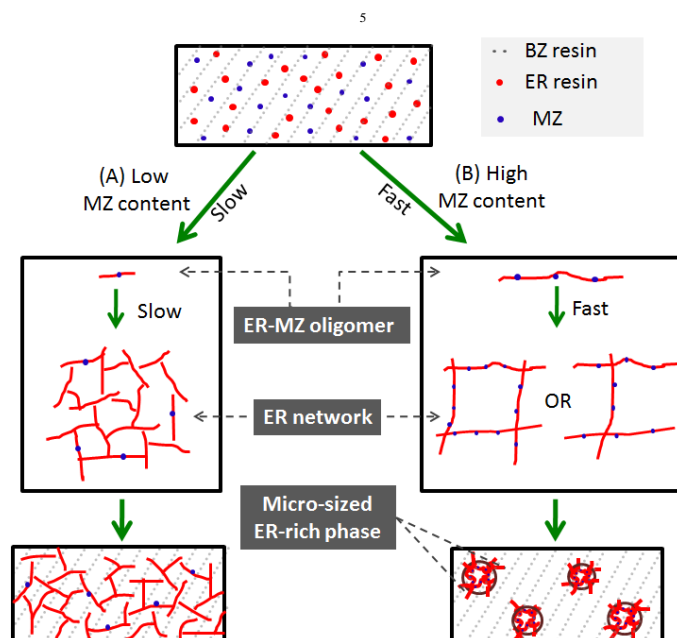


Figure 9. Rheological behavior of BZ/ER/MZ blending systems with (a) 3wt%, (b) 8wt% and (c) 12wt% of MZ upon curing at 110 °C as a function of time (s): (A) storage modulus (G' , solid line) and loss modulus (G'' , dash line), (B) Complex viscosity.

Scheme 3. Schematic of the relationship among MZ content, curing reaction and phase separation of BZ/ER/MZ blends at 110 °C.

ER. In this case, at the beginning, the slowly polymerization of ER/MZ neither enlarged the dynamic asymmetry between BZ and ER, nor effectively reduced the systemic entropy. And in the later stage, the formation of the highly crosslinked ER networks led to the increase of viscosity and the reduction of the mobility of ER network, thus inhibited the separation of ER network from the BZ matrix. Consequently, during the whole polymerization process, phase separation was impossible and only homogeneous structure was obtained.

(B) If the MZ content was high enough ($\geq 8\text{wt}\%$), the polymerization rate of ER was fast, and the molecular chain of ER-MZ oligomer was much longer. In this case, the dynamic asymmetry between ER-network and BZ resin was enlarged, and the system entropy was reduced sharply. Both of those led to the decrease of the compatibility of the ER polymer with surrounding BZ resin. In the late stage, the formation of branched or looser ER-network led to a relative low systemic viscosity, which allowed the free diffusion of BZ resin out from ER network. During this process, lightly crosslinked ER network gradually shrunk to exclude the entrapped BZ molecules due to its viscoelastic property, and finally micro-sized dispersed ER-rich phases were obtained.

4 Conclusions

In BZ/ER/MZ blending systems, the curing reaction of BZ/ER/MZ blend at 110 °C was mainly associated with the polymerization of ER with MZ. Increasing the MZ content could accelerate the polymerization of ER and enlarge the reactivity difference (ΔE_a) between ER and BZ resin, therefore reduced the possibility of copolymerization between BZ and ER. What's more, increase the MZ content led to the linear growth of the ER molecular chains and resulted in a looser network structures, which could not only increase the dynamic asymmetry between

BZ and ER, but also retain the system viscosity in a relative low range, therefore was the key to prepare multiphase structures in BZ/ER/MZ blend. That's why 0.8~1.2 μm sized sea-island phase structures were observed in BZ/ER/MZ blending with 8wt% and 12wt% of MZ systems but not in with 3wt% of MZ system. The final mechanical properties, especially the toughness of the BZ/ER/MZ blends will be systematically and deeply investigated in the future studies.

Acknowledgement

Supports for this project were provided by the National Natural Science Foundation of China (Project No. 50873062) and Doctoral Fund of Ministry of Education of China (Project No. 20090181110030).

Notes and references

- * College of Polymer Sciences and Engineering, State Key Laboratory of Polymer Materials Engineering, Sichuan University, Chengdu, China. Fax: 86-28-85405138; Tel: 86-28-85405138; E-mail: guyi@scu.edu.cn
- † Electronic Supplementary Information (ESI) available: [The fitted peak temperature (Table S1) and the Ozawa plots of $\ln\beta$ vs. $1/T$ for fitted Peak2 and Peak3 (Figure S1) of BZ/ER/MZ blends]. See DOI: 10.1039/b000000x/
- [1] J. P. Pascault, H. Sautereau, J. Verdu and R. J. J. Williams, *Thermosetting polymers*, Marcel Dekker: New York, 2002; chapter 1, 12-15.
 - [2] A. Gardziella, L. A. Pilato and A. Knop, *Phenolic Resins: Chemistry, Applications, Standardization, Safety and Ecology*, 2nd ed.; Springer: Berlin, 2000; chapter 6.
 - [3] J. B. Cho, J. W. Hwang, K. Cho, J. H. An and C. E. Park, *Polymer*, 1993, **34**, 4832.
 - [4] D. Klemperer, L. H. Sperling and L. A. Utracki, *Interpenetrating Polymer Networks*, 1st ed.; American Chemical Society: Washington, 1994; chapter 1.
 - [5] J. P. Pascault and R. J. J. Williams, In *Polymer blends*, Vol. 1:

- Formulation, Paul, D. R., Bucknall, C. B., Eds.; Wiley: New York, 2000; chapter 13, 379-415.
- [6] S. Thomas, A. Boudenne, L. Ibos and Y. Candau, In *Handbook of multiphase polymer systems*, 1st ed.; Boudenne, A., Ibos, L., Candau, Y., Thomas, S., Eds.; Wiley: United Kingdom, 2011; Vol. 1, p 1-12.
- [7] R. J. J. Williams, B. A. Rozenberg and J. P. Pascault, *Adv. Polym. Sci.*, 1997, **128**, 95.
- [8] Y. S. Kim and S. C. Kim, *Macromolecules*, 1999, **32**, 2334.
- [9] H. Kim and K. Char, *Ind. Eng. Chem. Res.*, 2000, **39**, 955.
- [10] Z. Wang, Q. Ran, R. Zhu and Y. Gu, *RSC Adv.*, 2013, **3**, 1350.
- [11] W. J. Gan, Y. F. Yu, M. H. Wang, Q. S. Tao and S. J. Li, *Macromolecules*, 2003, **36**, 7746.
- [12] H. Lü and S. Zheng, *Polymer*, 2003, **44**, 4689.
- [13] H. Ishida and D. J. Allen, *Polymer*, 1996, **37**, 4487.
- [14] J. Yang, M. A. Winnik, D. Ylitalo and R. J. DeVoe, *Macromolecules*, 1996, **29**, 7047.
- [15] K. Dean and W. D. Cook, *Macromolecules*, 2002, **35**, 7942.
- [16] Y. S. Yang and L. J. Lee, *Macromolecules*, 1987, **20**, 1490.
- [17] C. Jubsilp and S. Rimdusit, In *Handbook of benzoxazine resins*, 1st ed.; Ishida, H., Agag, T., eds.; Elsevier: Amsterdam, 2011; chapter 7, 169-172.
- [18] S. Rimdusit and H. Ishida, *Polymer*, 2000, **41**, 7941.
- [19] S. Rimdusit and H. Ishida, *J. Polym. Sci., Part B: Polym. Phys.*, 2000, **38**, 1687.
- [20] M. A. Espinosa, V. Cadiz and M. Galia, *J. Polym. Sci., Part A: Polym. Chem.*, 2004, **42**, 279.
- [21] N. N. Ghosh, B. Kiskan and Y. Yagci, *Prog. Polym. Sci.*, 2007, **32**, 1344-1391.
- [22] R. Jain, A. K. Narula and V. Choudhary, *J. Appl. Polym. Sci.*, 2007, **106**, 3327.
- [23] S. Mortimer, A. J. Ryan and J. L. Stanford, *Macromolecules*, 2001, **34**, 2973.
- [24] I. Glavchev, K. Petrova and I. Devedjiev, *Polym. Test*, 2002, **21**, 89.
- [25] M. Ghaemy and S. Sadiady, *Iran. Polym. J.*, 2006, **15**, 103.
- [26] Y. R. Ham, S. H. Kim, Y. J. Shin, D. H. Lee, M. Yang, J. H. Min and J. S. Shin, *J. Ind. Eng. Chem.*, 2010, **16**, 556.
- [27] S. K. Ooi, W. D. Cook, G. P. Simon and C. H. Such, *Polymer*, 2000, **41**, 3639.
- [28] L. S. Xu and J. R. Schlup, *J. Appl. Polym. Sci.*, 1998, **67**, 895.
- [29] B. Bilyeu, W. Brostow and K. Menard, US Pat, 7 868 067 B2, 2011.
- [30] B. N. Burns, H. Woolfson, P. Malone and J. Wigham, US Pat, 6 872 762 B2, 2005.
- [31] Y. X. Wang and H. Ishida, *Polymer*, 1999, **40**, 4563.
- [32] S. Atsushi, K. Ryoichi, N. Hiroshi, A. Kazuya and E. Takeshi, *Macromolecules*, 2008, **41**, 9030.
- [33] T. Agag, C. R. Arza, F. H. J. Maurer and H. Ishida, *Macromolecules*, 2012, **43**, 2748.
- [34] S. Grishchuk, Z. Mbhele, S. Schmitt and J. Karger-Kocsis, *eXPRESS Polym. Lett.*, 2011, **5**, 273.
- [35] H. Ishida and Y. Rodriguez, *Polymer*, 1995, **36**, 3151.
- [36] J. Dunkers and H. Ishida, *J. Polym. Sci., Part A: Polym. Chem.*, 1999, **37**, 1913.
- [37] K. Naoki and M. Schozo, JP Pat, 191775, 2000.
- [38] B. S. Rao, K. R. Reddy, S. K. Pathak and A. R. Pasala, *Polym. Int.*, 2005, **54**, 1371.
- [39] S. Rimdusit, S. Pirstpindvong, W. Tanthapanichakoon, S. Damrongsakkul, *Polym. Eng. Sci.*, 2005, **45**, 288.
- [40] H. Kimura, Y. Murata, A. Matsumoto, K. Hasegawa, K. Ohtsuka and A. Fukuda, *J. Appl. Polym. Sci.*, 1999, **74**, 2266.
- [41] H. Kimura, A. Matsumoto and K. Ohtsuka, *J. Appl. Polym. Sci.*, 2008, **109**, 1248.
- [42] H. Kimura, A. Matsumoto and K. Ohtsuka, *J. Appl. Polym. Sci.*, 2009, **112**, 1762.
- [43] B. S. Rao and S. K. Pathak, *J. Appl. Polym. Sci.*, 2006, **100**, 3956.
- [44] S. Grishchuk, S. Schmitt, O. C. Vorster and J. Karger-Kocsis, *J. Appl. Polym. Sci.*, 2012, **124**, 2824.
- [45] H. Wang, P. Zhao, H. Ling, Q. Ran and Y. Gu, *J. Appl. Polym. Sci.*, 2013, **127**, 2169.
- [46] P. Zhao, Q. Zhou, Y. Deng, R. Zhu and Y. Gu, *RSC Adv.*, 2014, **4**, 238.
- [47] H. Xiang, H. Ling, J. Wang, L. Song and Y. Gu, *Polym. Compos.*, 2005, **26**, 563.
- [48] A. A. Donatelli, L. H. Sperling and D. A. Thomas, *Macromolecules*, 1976, **9**, 671-675.
- [49] C. Jubsilp, S. Damrongsakkul, T. Takeichi and S. Rimdusit, *Thermochim. Acta*, 2006, **447**, 131.
- [50] R. Serra, J. Sempere and R. Nomen, *Thermochim. Acta*, 1998, **316**, 37.
- [51] A. K. Higham, L. A. Garber, D. C. Latshaw, C. K. Hall, J. A. Pojman and S. A. Khan, *Macromolecules*, 2014, **47**, 821.
- [52] M. S. Heise and G. C. Martin, *J. Appl. Polym. Sci.*, 1990, **39**, 721.
- [53] M. S. Heise and G. C. Martin, *Macromolecules*, 1989, **22**, 99.
- [54] J. Vogt, *J. Adhesion*, 1987, **22**, 139.
- [55] A. Farkas and P. F. Strohm, *J. Appl. Polym. Sci.*, 1968, **12**, 159.
- [56] J. M. Barton and P. M. Shepherd, *Die makromolekulare Chemie*, 1975, **176**, 919.
- [57] L. Weng, M. Chen and W. Chen, *Biomacromolecules*, 2007, **8**, 1109.
- [58] T. A. Ozawa, *Bull. Chem. Soc. Jpn.*, 1965, **38**, 1881.